Hindawi
Advances in Polymer Technology
Volume 2020, Article ID 1796701, 7 pages
https://doi.org/10.1155/2020/1796701

Research Article

Effects of Ginsenoside Biopolymer Nanoparticles on the Malignant Behavior of Non-Small-Cell Lung Cancer

Weizheng Zhou,[1] Chengliang Cai,[1] Hui Shi,[2] Hai Jin,[1] and Xiaowei Wang[1]

[1]*Department of Thoracic Surgery, Changhai Hospital, Shanghai 200435, China*
[2]*Department of Respiratory, Changhai Hospital, Shanghai 200435, China*

Correspondence should be addressed to Hai Jin; projinhai@163.com and Xiaowei Wang; xiaoweiwang@genopub.com

Received 22 October 2019; Revised 4 December 2019; Accepted 12 December 2019; Published 3 January 2020

Guest Editor: Mingqiang Li

Objective. To explore the effects and mechanism of ginsenoside Rg3 nanoparticles on the malignant behavior of non-small-cell lung cancer. *Methods*. The nanoparticle carriers were prepared by using an electrostatic system, and the coverage of ginsenoside Rg3 was determined by HPLC after coating the nanoparticle carriers with the ginsenoside Rg3 monomer. The proliferation of H125 cells was measured using MTT assay, and the Transwell assay was used to detect the invasiveness of H125 cells. Cell scratch test was used to determine the migration ability of H125 cells, and Western blotting was used to measure the expression level of PTEN in H125 cells; the expression level of miR-192 in H125 cells was measured via RT-qPCR, and the apoptosis level of H125 cells was detected by Tunel assay. *Results*. Firstly, gelatin nanoparticles and hyaluronic acid nanoparticles were uniformly distributed, uniform in size and spherical in shape, and after coating ginsenoside Rg3, the sizes of the nanoparticles were significantly increased. Secondly, the expression level of miR-192 was upregulated in H125 cells, which could be effectively inhibited by the treatment of Rg3 monomer and HA-Rg3 nanoparticles. Thirdly, the knockdown of miR-192 significantly inhibited H125 cell proliferation, invasion, and migration and also enhanced H125 cell apoptosis. In addition, PTEN was demonstrated as a target gene of miR-192. Finally, by inhibiting the expression level of miR-192 in H125 cells, the Rg3 monomer and HA-Rg3 nanoparticles upregulated the expression of PTEN and thus exerted its antitumor effect; the effects of HA-Rg3 were comparatively more significant than those of the Rg3 monomer. *Conclusions*. The Rg3 monomer and HA-Rg3 nanoparticles mitigated the malignant behavior of human non-small-cell lung cancer H125 cells through the miR-192/PTEN molecular axis, and HA-Rg3 nanoparticles showed better antitumor effects.

1. Introduction

With the aging of the population and the deterioration of the living environment, lung cancer has become one of the most common malignant tumors worldwide, and both morbidity and mortality are on the rise. It has become a malignant tumor with the highest morbidity and mortality in China with about 80% to 85% of them being non-small-cell lung cancer [1]. Ginsenoside Rg3 is one of the active ingredients in the ginseng extract. According to clinical evidence, ginsenoside Rg3 can inhibit malignant behaviors of tumors such as tumor invasion and metastasis, can alleviate the toxic effects of chemoradiotherapy, and also can sensitize tumors to antitumor drugs. However, the ginsenoside Rg3 monomer has low solubility in the human body, thus resulting in low effectiveness. Several studies indicated that the nanometer-sized particle carrier can improve the solubility of the drug, therefore increasing the body's absorption and improving the bioavailability of the drug.

MicroRNAs (miRNAs) are a class of noncoding single-stranded RNA molecules that affect various biological behaviors. The mechanism of action is mainly through the interaction with 3′-UTR to affect the mRNA expression of target genes. Many studies have shown that [2] the change of miRNA expression will lead to the upregulation or downregulation of its target gene mRNA expression and then affect cell proliferation and apoptosis. In addition, the abnormal expression of miRNAs can also induce a series of

human diseases, including cancer. Previous studies have shown that miR-192 expression is significantly increased in non-small-cell lung cancer tissues. It is thus speculated that miR-192 is related to the occurrence and development of non-small-cell lung cancer. The tumor suppressor gene phosphatase and tensin homolog (PTEN) is a dual-specific protein and lipid phosphatase, which can block the PI3K signaling pathway by activating AKT to inhibit cell proliferation and survival. Therefore, PTEN has a certain inhibitory effect on cancer [3]. Through prediction, it was found that PTEN may be a downstream target gene of miR-192. It is, therefore, speculated that miR-192 might affect the occurrence and development of non-small-cell lung cancer by regulating the expression of PTEN. Therefore, in this study, the nanoparticle carriers covered with ginsenoside Rg3 monomer were prepared to investigate its effect on the malignant behavior of human non-small-cell lung cancer cell line H125 and its underlying mechanism.

2. Material and Methods

2.1. Cell Lines and Reagents. In this study, human normal lung epithelial cells BEAS-2B were purchased from the Chinese Academy of Sciences Cell Bank, and human non-small-cell cancer cells H125 were purchased from FuHeng Cell Center, Shanghai, China. Ginsenoside Rg3 (Shenyi Capsule) was purchased from Jilin Yatai Pharmaceutical Co., Ltd.; fetal bovine serum and DMEM medium were purchased from Suzhou Laisa Biotechnology Co., Ltd.; the MTT kit was purchased from Beijing Kanglong Kangtai Biotechnology Co., Ltd.; the Transwell chamber was purchased from American BD Company; the Tunel kit and RIPA cell lysate were purchased from Shanghai Biyuntian Biotechnology Co., Ltd.; the Lipofectamine 2000 kit and reverse transcription kit were purchased from Shanghai Kemin Biotechnology Co., Ltd.; the ECL development kit was purchased from China Solarbio, and the dual-luciferase reporter gene detection kit was purchased from Beijing YuanPingHao Biotechnology Co., Ltd.

2.2. Preparation of Nanoparticles. Gelatin and hyaluronic acid nanoparticles were prepared in an electrostatic field preparation system. In addition, 4 μL of the prepared ginsenoside Rg3 solution (25 mg/mL) was separately added to 996 μL of prepared gelatin and hyaluronic acid nanoparticles (final concentration of ginsenoside Rg3 was 100 μg/mL) for their coating in the electrostatic field preparation system. The coverage of ginsenoside Rg3 was then determined by HPLC.

2.3. Cell Culture and Transfection. H125 cells were seeded in the DMEM medium (containing 10% fetal bovine serum, 100 U/L penicillin, and 100 mg/L streptomycin) and cultured in a constant temperature incubator at 37°C with 5% CO_2. miR-192 inhibitor, miR-NC, pc-PTEN, pc-NC, and sh-PTEN were provided by Shanghai Jima. The cells in the logarithmic growth phase were transfected with miRNA mimics and siRNAs according to the Lipofectamine 2000 kit. After 48 h of transfection, the cells were harvested for subsequent experiments. The primer sequences used in this study are shown in Table 1.

2.4. MTT Experiment. The single-cell suspension was prepared by trypsinization of H125 cells in the logarithmic growth phase. The cell concentration was adjusted to 5×10^3 cell/well and inoculated into a 96-well plate. The cells were then cultured in an incubator at 37°C with 5% CO_2. After 24 h, the cells were treated according to the experimental design and then cultured at 37°C with 5% CO_2 for 24 h. The cells were washed twice with PBS buffer solution and then cultured in a DMEM medium containing 10% fetal calf serum for 48 h. 20 μL (5 mg/L) MTT solution was added to each well, and the proliferation activity of H125 cells was measured in strict accordance with the instructions of the MTT kit.

2.5. Transwell Experiment. The upper chamber of the Transwell chamber was coated with Matrigel, and the H125 cells in the logarithmic growth phase were taken and seeded at a concentration of 1×10^5 cell/well in the upper chamber of the Transwell chamber containing a serum-free medium. The DMEM medium containing 10% fetal bovine serum was added to the lower chamber. The cells were removed 24 h after inoculation, fixed with formaldehyde, stained with crystal violet for 5 min, washed 3 times with PBS buffer, photographed, and counted.

2.6. Cell Scratch Test. 5×10^5 cells were added to each well of a 6-well plate. When the cell fusion rate reached 95%, the cell membrane was streaked and washed slowly with PBS buffer 3 times, the delineated cells were removed, and serum-free medium was added. The plate was incubated in a 37°C, 5% CO^2 incubator for 24 h and photographed after 24 h, and the scratch distance was determined using ImageJ.

2.7. Western Blotting. H125 cells were transferred to EP tubes, lysed on ice for 30 min using the RIPA cell lysate, and then centrifuged at 14,000 rpm for 5 min at 4°C. The supernatant was extracted and a loading buffer was added to the supernatant. The sample was then denatured at 100°C for 10 min and then stored at −20°C. 25 μg of protein sample was then loaded and electrophoresed at 40 A for 100 min. After that, it was then transferred to the membrane at 100 V for 90 min. After adding the primary antibody, the membrane was incubated at 4°C overnight and then incubated at room temperature for 2 h after the addition of the secondary antibody. Image development was performed strictly based on the ECL kit instructions and the grayscale analysis of protein bands was performed using ImageJ software.

2.8. RT-qPCR. H125 cellular RNA was extracted and 2 μL of the extracted RNA was added to 98 μL of ddH_2O to measure the RNA content and purity based on the absorbance value obtained through an ultraviolet spectrophotometer. The

Table 1: Primer sequences.

Gene name	Primer sequence
miR-192	5′-GGGCTGACCTATGAATTG-3′
	5′-CAGTGCGTGTCGTGGAGT-3′
U6	5′-ACGATGCACCTGTACGATCA-3′
	5′-TCTTTCAACACGCAGGACAG-3′

Table 2: RT-qPCR reaction system (20 μL).

Reagent	Volume (μL)
SYBR premix Ex Taq (2x)	10
Forward primer (5 pmol/L)	1
Reverse primer (5 pmol/L)	1
cDNA	0.5
RNase-FREE WATER	7.5

cDNA was then synthesized according to the instructions of the reverse transcription kit. The PCR reaction was carried out according to Table 2; specifically, the reaction conditions were as follows: 95°C, 10 min; 95°C, 20 s; 60°C, 1 min, for a total of 40 cycles.

2.9. Detection of Apoptosis by Tunel Assay. After the treated sample was rinsed with PBS buffer, the liquid surrounding the sample was removed. 100 μL of the TdT enzyme reaction solution was added to each sample, the reaction was carried out in the dark at 37°C for 60 min, and then the diluted SSC solution was added to terminate the reaction. After rinsing with PBS buffer, the samples were blocked in 0.3% hydrogen peroxide/PBS and incubated for 4 min at room temperature. 100 μL of the streptavidin-HRP working solution was then added, and the reaction was carried out at 37°C for 60 min. The BAD chromogenic solution was added, followed by rinsing the cells with PBS buffer 3 times, and then sealed with a neutral resin and observed under a microscope.

2.10. Dual-Luciferase Reporter Gene Assay. After the 3′-UTR fragment of PTEN gene was amplified and inserted into the double luciferase reporter gene plasmid, the positive clone was screened, followed by sequencing, amplification, and purification of the plasmid. The miR-192 plasmid and the empty vector were obtained in a similar manner. The plasmid of the reporter gene, miR-192, and empty vector were cotransfected with well-grown H125 cells, and the cells were then cultured in a constant temperature incubator at 37°C, with 5% CO_2 for 24 h. After that, the protein was purified, and the substrate was added; luciferase activities were measured by using a fluorescence counter.

2.11. Statistical Analysis. SPSS (version 22.0) statistical software was used for the data analysis, the data obtained in this study were expressed as $\overline{x} \pm s$, the t-test was used for comparison between groups, and the comparison among multiple groups was analyzed by one-way ANOVA. The difference was statistically significant when $P < 0.05$ or $P < 0.01$.

3. Results

3.1. Nanoparticle Detection and Vector Screening. The prepared gelatin nanoparticle carriers and hyaluronic acid nanoparticle carriers were found uniformly distributed, uniform in size and spherical in shape under the electron transmission microscopy, and the particle sizes of the nanoparticle carriers were 4.5 ± 0.75 nm and 16.4 ± 4.2 nm, respectively. As shown in Figures 1(a) and 1(b), the results of MTT experiments showed that cell viability of H125 cells was significantly reduced when cocultured with 20 μL gelatin nanoparticle carrier suspension ($P < 0.05$), while similar significantly reduced cell viability of H125 cells was observed, and when cocultured with 40 μL hyaluronic acid nanoparticle carrier suspension ($P < 0.05$). After coculture of H125 cells with gelatin polymer or HA polymer, the activity of H125 cells is similar to that of gelatin or HA nanoparticles; see Figure 1(c). After coating ginsenoside Rg3, Gelatin-Rg3 nanoparticles and hyaluronic acid HA-Rg3 nanoparticles showed a small amount of particle agglomeration, and the particle sizes of the nanoparticles were significantly different from that before coating ($P < 0.01$); the particle sizes were 40.3 ± 5.8 nm and 31.2 ± 8.4 nm, respectively. The coverage of ginsenoside Rg3 on gelatin and hyaluronic acid nanoparticles measured by HPLC was 13.715 ± 1.985% and 36.410 ± 6.472%, respectively. Therefore, to reduce the impact of nanoparticle carriers on H125 cells, HA-Rg3 nanoparticles were selected for subsequent experiments.

3.2. Effect of HA-Rg3 Bio-Polymerized Nanoparticles on the Expression Level of miR-192. As shown in Figure 2(a), the expression level of miR-192 in H125 cells was significantly higher than that of BEAS-2B cells. However, the expression levels of miR-192 in H125 cells were significantly downregulated after cocultured with ginsenoside Rg3 and HA-Rg3 bio-polymerized nanoparticles ($P < 0.05$), and the expression levels of miR-192 achieved lowest when H125 cells were cocultured with HA-Rg3 ($P < 0.01$) as shown in Figure 2(b).

3.3. Effect of miR-192 on Malignant Behavior of H125 Cells. The results of RT-qPCR showed that the expression level of miR-192 in H125 cells was significantly downregulated compared with the control group after the transfection of miR-192 inhibitor ($P < 0.01$), as shown in Figure 3. And the knockdown of miR-192 significantly inhibited the activity of H125 cells ($P < 0.01$) as shown in MTT (Figure 4(a)), significantly inhibited the invasion of H125 cells ($P < 0.05$) as shown in Transwell results (Figure 4(b)), and also significantly inhibited the migration ability of H125 cells ($P < 0.05$) as shown in the results of cell scratch assay (Figure 4(c)). Furthermore, knockdown of miR-192 also significantly promoted the apoptosis of H125 cells ($P < 0.01$) as shown in Figure 4(d).

3.4. PTEN Is the Target Gene of miR-192. By using the ENCORI database, we predicted that the 3′-UTR end of

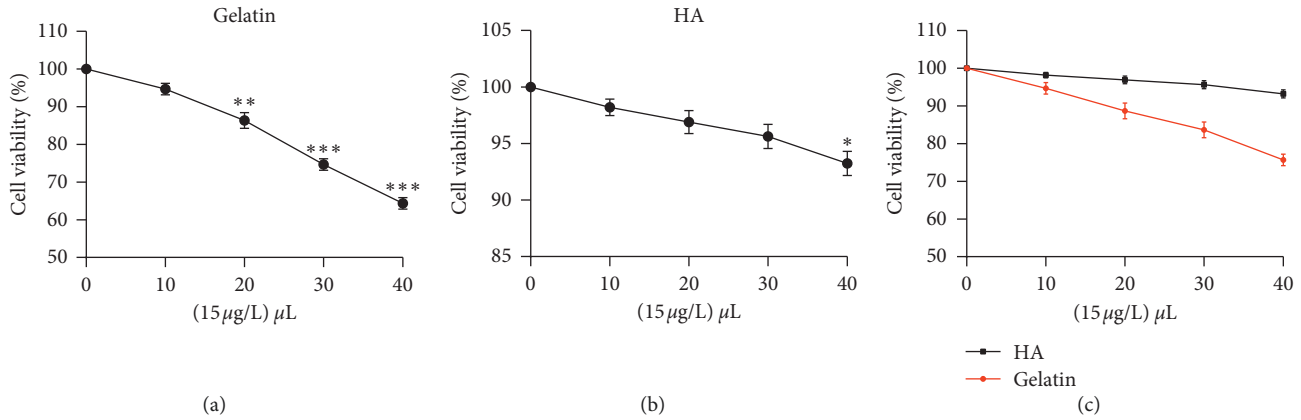

Figure 1: Nanoparticle detection and vector screening. (a, b) H125 cells proliferation activity. $^{*}P < 0.05$, $^{**}P < 0.01$, and $^{***}P < 0.001$ vs the 0 μL group.

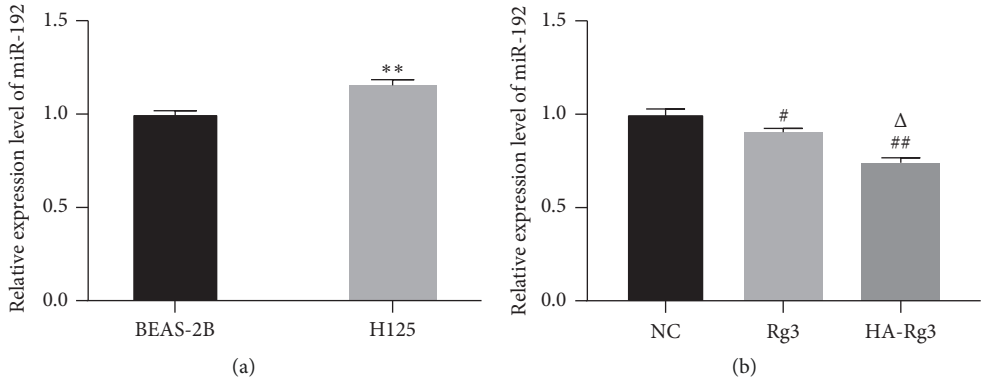

Figure 2: Effect of HA-Rg3 bio-polymerized nanoparticles on the expression level of miR-192. (a, b): The relative expression level of miR-192. $^{**}P < 0.01$ vs the BEAS-2B group; $^{\#}P < 0.05$ and $^{\#\#}P < 0.01$ vs the NC group; $^{\triangle}P < 0.05$ vs the NC group.

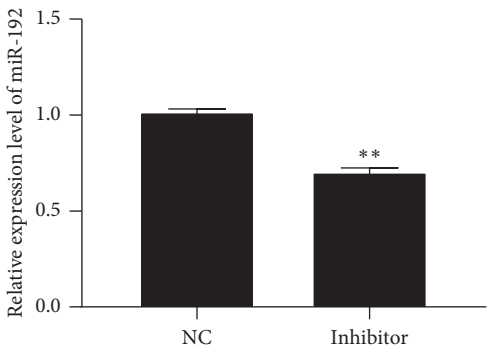

Figure 3: Effects of miR-192 on malignant behavior of H125 cells. $^{**}P < 0.01$ vs the NC group.

PTEN mRNA has a partial base sequence binding to the 5′-UTR end of miR-192 as shown in Figure 5(a). Western blotting results (Figure 5(b)) showed that the expression level of PTEN was significantly downregulated in H125 cells ($P < 0.05$), whereas the knockdown of miR-192 significantly enhanced the expression of PTEN in H125 cells ($P < 0.05$). Moreover, as shown in Figure 5(c), the results of the dual-luciferase assay verified that PTEN is the target gene of miR-192.

3.5. Mechanism of Action of HA-Rg3 Bio-Polymerized Nanoparticles on Non-Small-Cell Lung Cancer. The MTT assay showed that the proliferation activity of H125 cells in group I and group II was significantly lower than that in the NC group ($P < 0.01$), and the proliferation activity of H125 cells in group III and IV was significantly inhibited ($P < 0.001$), whereas the proliferation activity of H125 cells in the V group was not significantly different from that in the NC group. Moreover, the activity of H125 cells in group II was significantly inhibited when compared with group I ($P < 0.05$) as shown in Figure 4(a). Transwell results (Figure 4(b)) showed that the invasiveness of H125 cells in group I, II, III, and IV was inhibited compared with the NC group, and the difference was statistically significant ($P < 0.05$), whereas the invasion of H125 cells in group V was not significantly different from that of the NC group, and the invasiveness of H125 cells in group II was significantly lower than that of group I ($P < 0.05$). The scratch test results (Figure 4(c)) measuring the cell migration ability also showed that H125 cells in group I, II, III, and IV was inhibited compared with the NC group, and the difference was statistically significant ($P < 0.05$); the H125 cells in group V was not significantly different from that of the NC group, and the migration ability of H125 cells in group II was significantly lower than that of

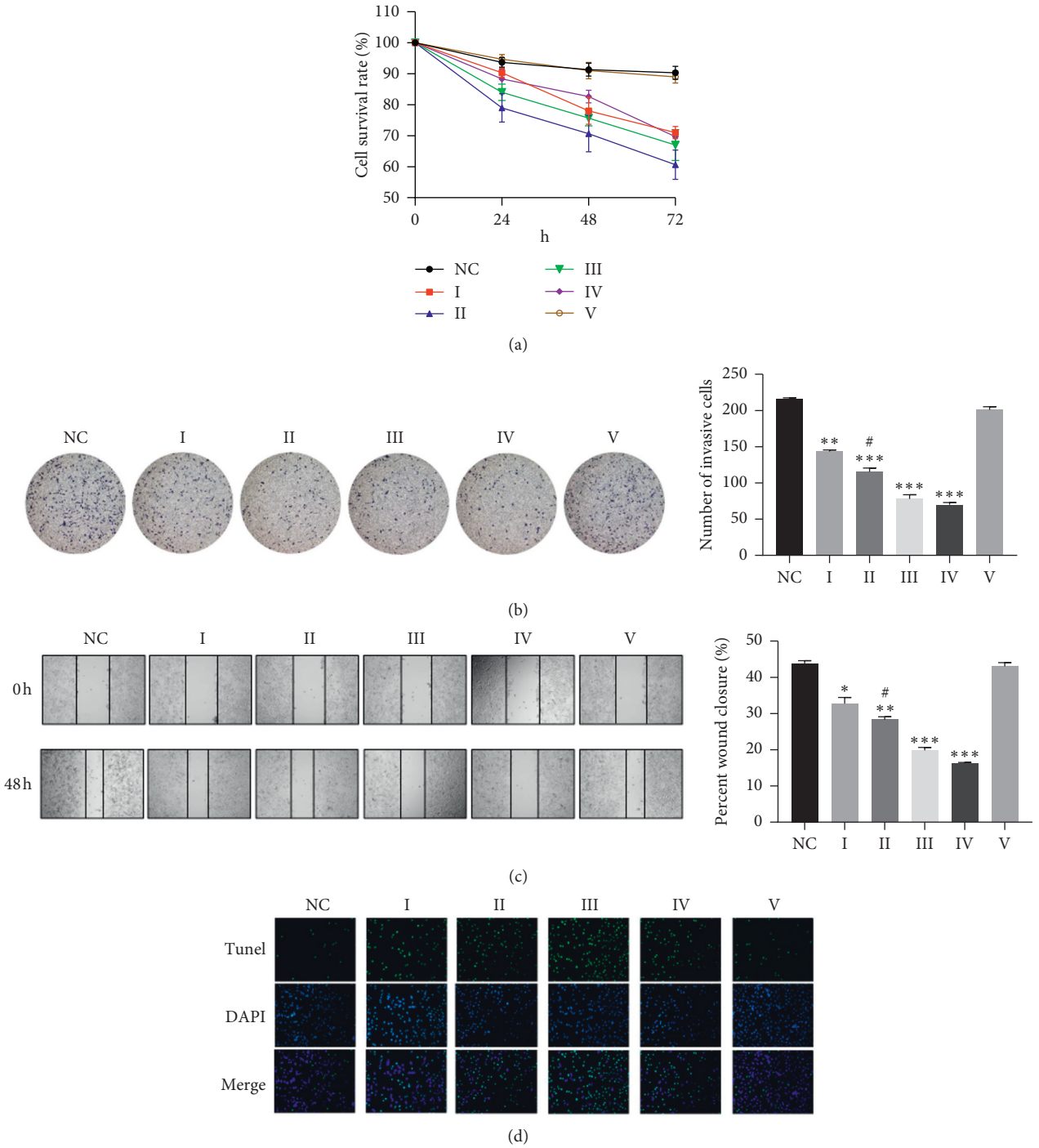

Figure 4: Mechanism of action of HA-Rg3 bio-polymerized nanoparticles on non-small-cell lung cancer. (a) H125 cells proliferation activity; (b) the invasion of H125 cells detected by Transwell assay; (c) the migration ability of H125 cells detected by wound healing; (d) the apoptosis of H125 cells was measured by Tunel assay. Groups (I) II, III, IV, and V were Rg3, HA-Rg3, miR-192 inhibitor, pc-PTEN, and miR-192 inhibitor + sh-PTEN, respectively. $^{**}P < 0.01$ vs the NC group.

group I ($P < 0.05$). The apoptosis results of Tunel assay (Figure 4(d)) showed that the number of apoptosis of H125 cells in group I, group II, group III, and group IV increased in different degrees compared with the NC group, and the difference was statistically significant ($P < 0.05$). There was no significant difference in the number of apoptosis of H125 cells in the V group compared with the NC group, and again the number of apoptosis of H125 cells in group II was significantly lower than that of group I ($P < 0.05$).

4. Discussion

Lung cancer is primary bronchial carcinoma, of which non-small-cell lung cancer is the most common type of cancer,

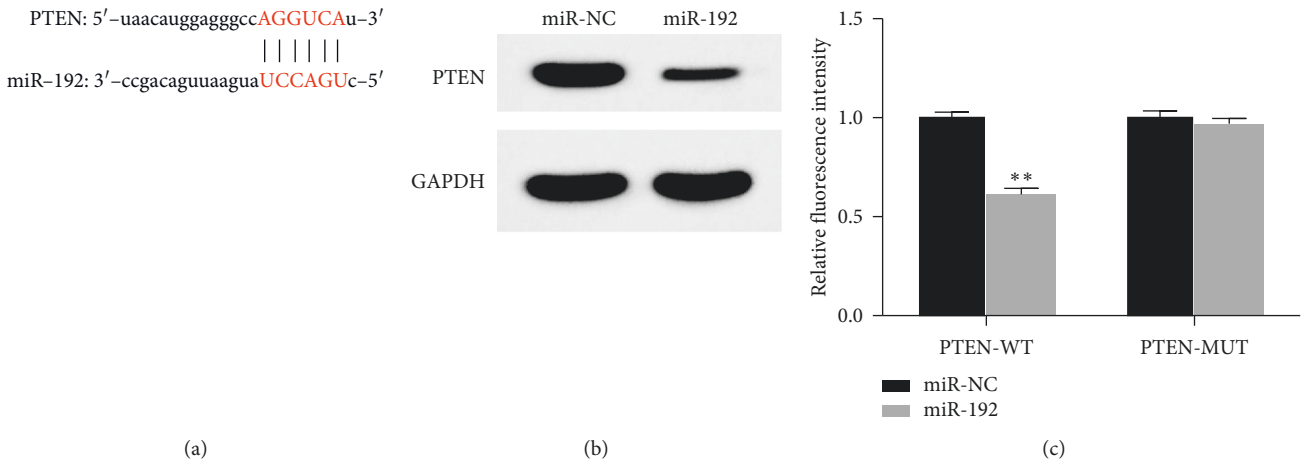

Figure 5: PTEN is the target gene of miR-192. (a) the predicted results of target genes; (b) detection of PTEN protein level by Western blotting; (c) detection of the Interaction between miR-192 and PTEN by DLRTM. $^{**}P < 0.01$ vs the miR-NC group.

accounting for 75% to 80% of the total number of lung cancer patients [4]. Due to the lack of early specific symptoms, lung cancer often develops into the advanced stage at the clinical diagnosis. Although surgery can be used to treat early-stage lung cancer, 70% of patients cannot be cured [4]. Recently, radiotherapy and chemotherapy are becoming mainstream methods for the treatment of lung cancer. However, with that comes the toxic side effects and higher recurrence rate, and it is also demanding in terms of the patient's physical quality. In recent years, the advantages of traditional Chinese medicine in cancer treatment have gradually gained attention, which can reduce the side effects of radiotherapy and chemotherapy on patients, prolong the quality lifespan of patients, and alleviate the drug resistance in the cancer treatments [5–7].

Ginsenoside Rg3 is the active ingredient extracted from ginseng. The main component of which is tetracyclic triterpenoid saponin, which can inhibit the formation of tumor blood vessels, block the invasion and metastasis of tumors, and improve the immunity and quality of life for the cancer patients. Wu et al. [8] reported that ginsenoside Rg3 can inhibit the proliferation of thyroid cancer in vitro and in vivo and significantly inhibit the metastasis of thyroid cancer. Dai et al. [5] showed that ginsenoside Rg3 could enhance the anticancer activity of gefitinib and enhance the sensitivity of non-small-cell lung cancer to gefitinib. At present, the "Senyi Capsule" containing ginsenoside Rg3 has been approved for marketing in China and has been used for clinical treatment of cancer, which has achieved a certain curative effect. However, the low solubility of monomeric ginsenoside Rg3 in the human body results in its low bioavailability thus its effectiveness. Because of the small particle diameter, the nanocarrier has been believed to be beneficial to increase the stability, solubility, and ultimately bioavailability of the drug in the human body. Studies have shown that biomimetic 50 nm nanoparticles coated with paclitaxel can prevent the drug from being absorbed by the normal lung cells of the human body because of its surface characteristics, which ultimately can more effectively deliver drugs and improve the bioavailability of the drug [9]. The results of our study showed that the hyaluronic acid nanoparticles coated with ginsenoside Rg3 showed better antitumor effect in vitro, compared with ginsenoside Rg3 monomer. It also more effectively inhibited the proliferation, invasion, and migration of H125 cells as well as promoting the apoptosis of H125 cells. Although ginsenoside Rg3 has certain antitumor curative effects, its mechanism of action has not yet been fully understood. Therefore, it is necessary and urgent to explore the mechanism of action of ginsenoside Rg3 and its biopolymer nanoparticles on non-small-cell lung cancer.

MicroRNAs (miRNAs) are a class of noncoding single-stranded RNA molecules consisting of approximately 22 nucleotides that regulate the expression of proteins in plants and animals. Studies have shown the abnormal expression of various miRNAs in cancer tissues or patients' serum. For example, the expression level of miR-125b in patients' serum can be used as a biomarker for the diagnosis and prognosis of epithelial ovarian cancer [10]. The expression levels of miR-21-5p, miR-141-3p, and miR-205-5p in urine can be used as biomarkers for the diagnosis of prostate cancer and bladder cancer [11]. By reviewing the literature, miR-192 was found upregulated in non-small-cell lung cancer and can be used as a biomarker for the diagnosis of non-small-cell lung cancer [12]. By summarizing the literature reviewed, it is speculated that miR-192 can affect various biological behaviors in H125 cells by regulating PTEN expression. The results in this study showed that the expression of miR-192 was upregulated in H125 cells and the knockdown of miR-192 significantly inhibited the malignant biological behavior of H125 cells. By double luciferase reporter gene experiments, PTEN was revealed as a downstream target of miR-192.

In summary, HA-Rg3 nanoparticles have more advantages in inhibiting H125 cell proliferation, invasion, migration, and promoting H125 cell apoptosis than monomeric ginsenoside Rg3. Further research indicates that ginsenoside Rg3 monomer and HA-Rg3 nanoparticles may inhibit non-small-cell lung cancer by downregulating the

expression level of miR-192 in H125 cells and thus promoting the expression of PTEN in H125 cells.

Data Availability

The data used to support the findings of this study are included within the article.

Conflicts of Interest

The authors declare that they have no conflicts of interest.

Authors' Contributions

Weizheng Zhou and Chengliang Cai contributed equally to this study.

Acknowledgments

This work was funded by the Wu Jieping Medical Fund (no. 320.6750.12213).

References

[1] N. Shriwash, P. Singh, S. Arora, M. Ali, S. Ali, and R. Dohare, "Identification of differentially expressed genes in small and non-small cell lung cancer based on meta-analysis of mRNA," *Heliyon*, vol. 5, no. 6, Article ID e01707, 2019.

[2] A. Lujambio and S. W. Lowe, "The microcosmos of cancer," *Nature*, vol. 482, no. 7385, pp. 347–355, 2012.

[3] B. D. Hopkins, C. Hodakoski, D. Barrows, S. M. Mense, and R. E. Parsons, "PTEN function: the long and the short of it," *Trends in Biochemical Sciences*, vol. 39, no. 4, pp. 183–190, 2014.

[4] R. L. Siegel, K. D. Miller, and A. Jemal, "Cancer statistics, 2017," *CA: A Cancer Journal for Clinicians*, vol. 67, no. 1, pp. 7–30, 2017.

[5] Y. Dai, W. Wang, Q. Sun, and J. Tuohayi, "Ginsenoside Rg3 promotes the antitumor activity of gefitinib in lung cancer cell lines," *Experimental and Therapeutic Medicine*, vol. 17, no. 1, pp. 953–959, 2018.

[6] X.-J. Wang, R.-J. Zhou, N. Zhang, and Z. Jing, "20 (S)-ginsenoside Rg3 sensitizes human non-small cell lung cancer cells to icotinib through inhibition of autophagy," *European Journal of Pharmacology*, vol. 850, pp. 141–149, 2019.

[7] Y. Zhang, X. Q. Wang, H. Liu et al., "A multicenter, large-sample, randomized clinical trial on improving the median survival time of advanced non-small cell lung cancer by combination of Ginseng Rg3 and chemotherapy," *Zhonghua Zhong Liu Za Zhi*, vol. 40, no. 4, pp. 295–299, 2018.

[8] W. Wu, Q. Zhou, W. Zhao et al., "Ginsenoside Rg3 inhibition of thyroid cancer metastasis is associated with alternation of actin skeleton," *Journal of Medicinal Food*, vol. 21, no. 9, pp. 849–857, 2018.

[9] H. Choi, T. Liu, H. Qiao et al., "Biomimetic nano-surfactant stabilizes sub-50 nanometer phospholipid particles enabling high paclitaxel payload and deep tumor penetration," *Biomaterials*, vol. 181, pp. 240–251, 2018.

[10] M. Zuberi, I. Khan, R. Mir, G. Gandhi, P. C. Ray, and A. Saxena, "Utility of serum miR-125b as a diagnostic and prognostic indicator and its alliance with a panel of tumor suppressor genes in epithelial ovarian cancer," *PLoS One*, vol. 11, no. 4, Article ID e0153902, 2016.

[11] N. Ghorbanmehr, S. Gharbi, E. Korsching, M. Tavallaei, B. Einollahi, and S. J. Mowla, "miR-21-5p, miR-141-3p, and miR-205-5p levels in urine-promising biomarkers for the identification of prostate and bladder cancer," *The Prostate*, vol. 79, no. 1, pp. 88–95, 2019.

[12] X. Du, F. Qi, S. Lu, Y. Li, and W. Han, "Nicotine upregulates FGFR3 and RB1 expression and promotes non-small cell lung cancer cell proliferation and epithelial-to-mesenchymal transition via downregulation of miR-99b and miR-192," *Biomedicine & Pharmacotherapy*, vol. 101, pp. 656–662, 2018.